



# Dayside and nightside contributions to the cross polar cap potential: placing an upper limit on a viscous-like interaction

S. E. Milan

## ► To cite this version:

S. E. Milan. Dayside and nightside contributions to the cross polar cap potential: placing an upper limit on a viscous-like interaction. *Annales Geophysicae*, 2004, 22 (10), pp.3771-3777. hal-00317725

**HAL Id: hal-00317725**

**<https://hal.science/hal-00317725>**

Submitted on 3 Nov 2004

**HAL** is a multi-disciplinary open access archive for the deposit and dissemination of scientific research documents, whether they are published or not. The documents may come from teaching and research institutions in France or abroad, or from public or private research centers.

L'archive ouverte pluridisciplinaire **HAL**, est destinée au dépôt et à la diffusion de documents scientifiques de niveau recherche, publiés ou non, émanant des établissements d'enseignement et de recherche français ou étrangers, des laboratoires publics ou privés.

# Dayside and nightside contributions to the cross polar cap potential: placing an upper limit on a viscous-like interaction

S. E. Milan

Department of Physics and Astronomy, University of Leicester, Leicester LE1 7RH, UK

Received: 10 June 2004 – Revised: 1 July 2004 – Accepted: 15 July 2004 – Published: 3 November 2004

**Abstract.** Observations of changes in size of the ionospheric polar cap allow the dayside and nightside reconnection rates to be quantified. From these it is straightforward to estimate the rate of antisunward transport of magnetic flux across the polar regions, quantified by the cross polar cap potential  $\Phi_{PC}$ . When correlated with upstream measurements of the north-south component of the IMF,  $\Phi_{PC}$  is found to increase for more negative  $B_z$ , as expected. However, we also find that  $\Phi_{PC}$  does not, on average, decrease to zero, even for strongly northward IMF. In the past this has been interpreted as evidence for a viscous interaction between the magnetosheath flow and the outer boundaries of the magnetosphere. In contrast, we show that this is the consequence of flows excited by tail reconnection, which is inherently uncorrelated with IMF  $B_z$ .

**Key words.** Ionosphere (plasma convection) – Magnetospheric physics (magnetospheric configuration and dynamics; auroral phenomena)

## 1 Introduction

It has been known for several decades that the level of geomagnetic activity is enhanced when the interplanetary magnetic field (IMF) is directed southwards, that is, when IMF  $B_z < 0$  nT (e.g. Fairfield and Cahill, 1966). This was put forward as evidence that magnetic reconnection between the IMF and the northwards-directed field of the sub-solar magnetopause was responsible for coupling energy, mass, and momentum from the solar wind into the magnetosphere, as first proposed by Dungey (1961, 1963). It was also demonstrated that the ionospheric convection flow rate, quantified by the “cross polar cap potential” or  $\Phi_{PC}$ , is approximately proportional to  $B_s$ , where  $B_s = |B_z|$  for  $B_z < 0$  nT (e.g. Reiff et al., 1981, 1985; Cowley, 1984; Weimer, 2001), though perhaps 50–100 kV, on average. When the IMF  $B_z > 0$  nT ( $B_s = 0$  nT) then sub-solar reconnection is expected to cease, and it was thought that  $\Phi_{PC}$  should tend to zero. However,

as noted by Reiff et al. (1981, 1985) and Weimer (2001), under such situations the cross polar cap potential remains non-zero, taking an average value of a few 10 s of kV. As reconnection was not the favoured mechanism for maintaining this “ground state” ionospheric convection, a viscous interaction between the antisunwards flow of the magnetosheath and the flanks of the magnetosphere was invoked instead, as first proposed by Axford and Hines (1961). This idea became incorporated into theoretical models of the expected ionospheric flow (e.g. Cowley and Lockwood, 1992), though perhaps there has been scant evidence for the existence of such “viscous cells” in empirically determined convection patterns (e.g. Heppner and Maynard, 1987; Ruohoniemi and Greenwald, 1996; Weimer, 1995, 2001). The present paper seeks to demonstrate that no such interaction is necessary to explain the observations, or that at least an upper limit can be placed on the viscous contribution to the convection pattern. Instead, we show that the cross polar cap potential is made up of contributions from two independent processes, not only sub-solar (dayside) reconnection but also magnetotail (nightside) reconnection, sometimes described as the “expanding/contracting polar cap model” (Russell, 1972; Siscoe and Huang, 1985; Holzer et al., 1986; Lockwood et al., 1990; Lockwood, 1991; Lockwood and Cowley, 1992; Cowley and Lockwood, 1992). These two components can loosely be identified with the “directly-driven” and “loading-and-unloading” paradigms discussed extensively in the past (e.g. Rostoker et al., 1987; Baker et al., 1997). Dayside reconnection is directly controlled by the upstream solar wind conditions; nightside reconnection is not. As suggested by Lockwood et al. (1990), it is this nightside reconnection which maintains the non-zero ground-state convection, even after dayside reconnection has ceased.

## 2 Day- and nightside reconnection and the cross polar cap potential

The rate of change of open flux in the magnetosphere is determined by the competition between the rates of dayside and

Correspondence to: S. Milan  
(steve.milan@ion.le.ac.uk)

nightside reconnection, as described by the following statement of Faraday's Law:

$$\frac{d}{dt} \int_{PC} \mathbf{B} \cdot d\mathbf{s} = \frac{dF_{PC}}{dt} = \Phi_D - \Phi_N, \quad (1)$$

where  $\mathbf{B}$  is the magnetic field strength at ionospheric altitudes,  $F_{PC}$  is the flux contained in the polar cap, and  $\Phi_D$  and  $\Phi_N$  are the rates (voltages) of creation and destruction of open flux at the low-latitude dayside magnetopause and in the magnetotail, respectively (e.g. Siscoe and Huang, 1985; Holzer et al., 1986; Lockwood and Freeman, 1989; Lockwood, 1991). It is also this dayside and nightside reconnection which leads to the general transport of plasma and flux antisunward across the polar cap, and it is this transport that the polar cap potential  $\Phi_{PC}$  is intended to quantify. Perhaps one of the greatest obstacles to the study of the response of ionospheric convection to solar wind-magnetosphere coupling is the lack of standardization of the definition of  $\Phi_{PC}$ , which is expressed as a voltage: the convection electric field integrated along a representative cut across the polar regions. However, the exact value of  $\Phi_{PC}$  depends on the start and end points of this cut (though not on the path chosen), and it is here that inconsistencies arise.

One method of measurement is the integration of the electric field measured by a polar-orbiting satellite as it traverses the convection pattern from dawn to dusk (or vice versa), specifically between the dawn and dusk convection reversal boundaries. In this method, an "ideal" pass of the polar regions could be defined as an orbit that follows the dawn-dusk meridian. If the polar cap remains approximately circular (though expanding or contracting in response to the accumulation or loss of open flux as described by Eq. (1)), then the rate of antisunward flux transport across this dawn-dusk meridian has been argued by Lockwood (1991) and Lockwood and Cowley (1992) to be given by

$$\Phi_{PC} = \frac{1}{2} (\Phi_D + \Phi_N) + \Phi_V. \quad (2)$$

Lockwood and Cowley (1992) included the voltage associated with a viscous interaction as  $\Phi_V$ , though this was omitted by Lockwood (1991), or, in other words, they assumed that  $\Phi_V=0$ .

A second method of measuring the cross polar cap potential is to fully determine the electrostatic potential pattern associated with the convection (using a technique such as AMIE (Richmond and Kamide, 1988) or SuperDARN "map-potential" (Ruohoniemi and Baker, 1998)) and then set  $\Phi_{PC}$  equal to the difference between the maximum and minimum of the potential. In this case, we expect that  $\Phi_{PC}$  will be close to the dayside or nightside reconnection rate, depending on which is greatest:

$$\Phi'_{PC} = \left. \begin{array}{l} \Phi_D + \Phi_V \\ \Phi_N + \Phi_V \end{array} \right\} \begin{array}{l} \Phi_D > \Phi_N \\ \Phi_D < \Phi_N \end{array}. \quad (3)$$

In effect, this method chooses the representative cut of the polar cap to start and end near the extremities of the most active merging line. We note that great care should be taken

when comparing studies that have used different methods of determining the polar cap potential: Eq. (3) tends to give double the estimate of  $\Phi_{PC}$  of Eq. (2) (see below).

In this paper we quantify  $\Phi_D$  and  $\Phi_N$  from observations of the polar ionosphere, and use this to determine  $\Phi_{PC}$ . We favour the first method (Eq. (2)) of measuring  $\Phi_{PC}$ , as the previous studies with which we compare our observations used polar-orbiting spacecraft to measure the cross polar potential (though we also describe the outcome of employing Eq. (3)). The aim of the present paper is to determine whether  $\Phi_V$  is zero or non-zero, or at least to place an upper limit on  $\Phi_V$ , by comparing the relationship between  $\Phi_{PC}$  and IMF  $B_z$  with previous observations. To do this we assume that the viscous interaction is negligible ( $\Phi_V=0$ ), and demonstrate that even so we reproduce well previous measurements of  $\Phi_{PC}$ .

### 3 Methodology and observations

Recent studies have employed observations of the polar ionosphere to determine the quantity of open flux contained within the northern polar cap (Milan et al., 2003, 2004; Milan, 2004). Taken from these studies, Figs. 1c and g show the variation in open flux (grey lines) determined during two 8-hour intervals on 5 June and 26 August 1998. The corresponding lagged  $B_z$  component of the IMF, as measured by the Wind spacecraft, is shown in panels a and e. The polar cap appears to expand (the quantity of open flux increases) when the IMF is directed southwards ( $B_z < 0$  nT), and contracts following the onset of substorm break-ups (SB) or significant nightside auroral brightenings (AB), indicated by vertical dashed lines, deduced from magnetometer and auroral observations.

As proposed by Levy et al. (1964) and demonstrated by Holzer and Slavin (1979), Holzer et al. (1986), Milan (2004) and Milan et al. (2004), the dayside reconnection rate can be approximated by

$$\Phi_D \approx -LV_x B_s, \quad (4)$$

where  $V_x$  is the  $X$ -component of the solar wind flow (negative antisunward, hence the minus sign in Eq. (4) to make  $\Phi_D$  positive) such that  $-V_x B_s$  is the (half-wave rectified)  $Y$ -component of the solar wind electric field, and  $L$  is a characteristic scale length of the order of 5–8  $R_E$  which can be thought of as the effective cross section presented by the magnetosphere to the impinging solar wind. The actual cross-wind scale size of the magnetosphere is approximately 25–30  $R_E$ , so the reconnection efficiency can be considered to be  $\sim 0.2$ , as also found by Holzer et al. (1986). Note that in Eq. (4) we implicitly set  $\Phi_D$  to zero when the IMF is directed northwards, as we do not expect low-latitude reconnection to occur under these circumstances.

Panels b and f show the dayside reconnection rate  $\Phi_D$  predicted from Eq. (2), using values of  $L$  of 5 and 8 in the two examples, respectively. These values of  $L$  were selected to match the rate of polar cap expansion during periods when

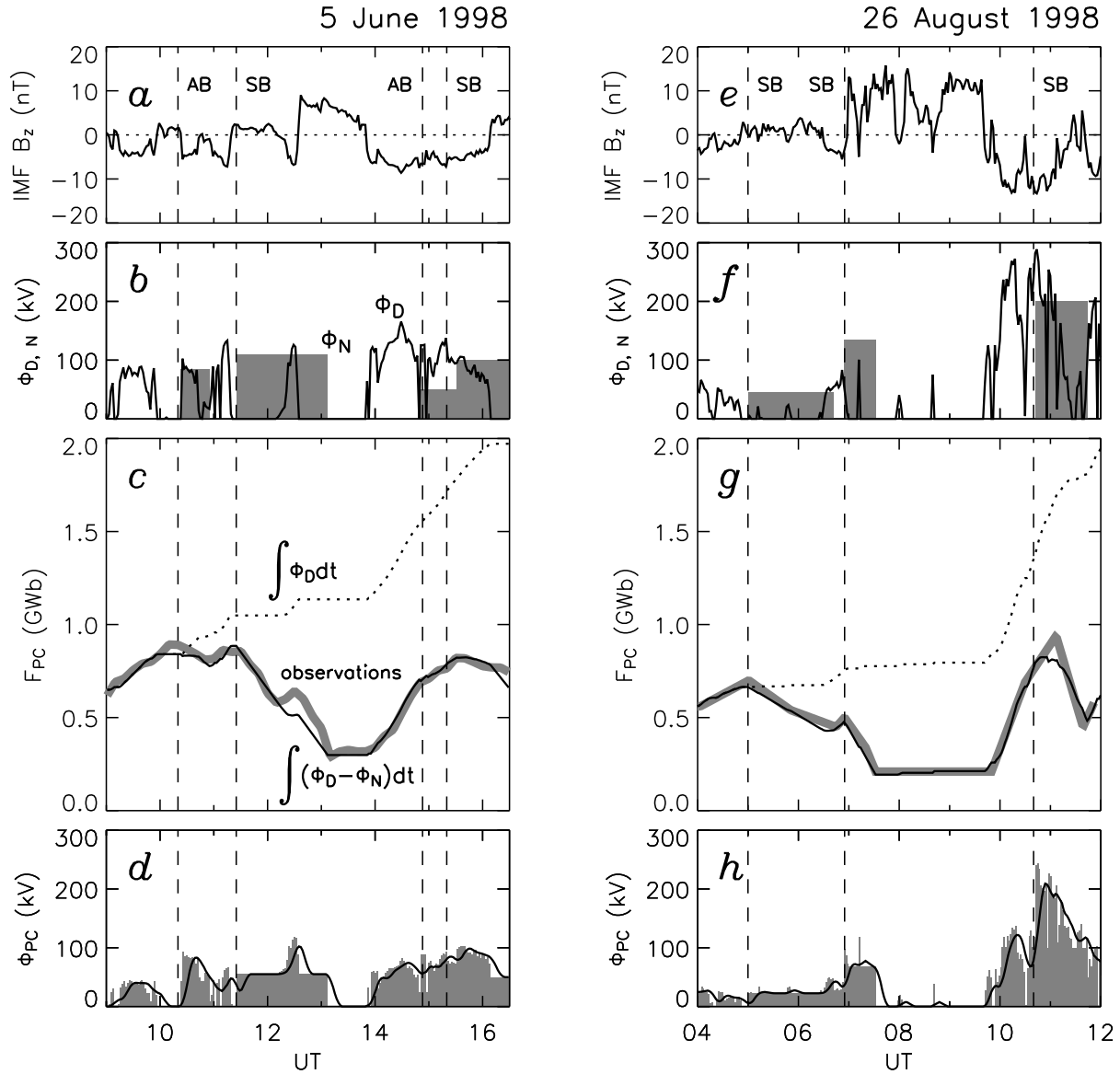


**Fig. 1.** Observations of changes in polar cap flux and deduced rates of dayside and nightside reconnection for two 8-hour intervals on 5 June and 26 August 1998. (a, e) IMF  $B_z$  lagged to the magnetopause. (b, f) Deduced rates of day- (solid curve) and nightside (grey blocks) reconnection. (c, g) Variation in polar cap flux (grey curve), modeled polar cap flux derived from integration of dayside reconnection rate (dotted curve) and modeled polar cap flux including fitted nightside reconnection (solid curve). (d, h) Cross polar cap potential derived from day- and nightside reconnection rates (grey), and smoothed with a triangular response function (solid curve).

tail reconnection is thought to be inactive. Panels c and g show the corresponding predicted increase in polar cap flux  $F_{PC}$  (dotted curve). This predicted  $F_{PC}$  is set equal to the observed polar cap flux at the start of the interval, and from then on is calculated by the integration of  $\Phi_D$ , that is assuming that  $\Phi_N=0$  in Eq. (1). The predicted flux and observed flux match each other well initially, but begin to deviate after the first substorm or auroral brightening, indicating the onset of tail reconnection (of open flux), i.e.  $\Phi_N > 0$ . The level of tail reconnection can be estimated from the discrepancy between the predicted and observed  $F_{PC}$ . We find that the observations can be reproduced to a good accuracy by assuming

that tail reconnection commences promptly at substorm onset, and continues at a uniform rate for a set length of time, which differs in each case. These fits are indicated in panels b and f, and the resultant predicted variation of  $F_{PC}$ , that is the integration of  $\Phi_D - \Phi_N$ , is overlaid in panels c and g (full curves). Thus, we have estimates of both  $\Phi_D$  and  $\Phi_N$ . The observations provide a clear indication of the validity of the two-component coupling process or “expanding/contracting polar cap” model.

It is then possible to estimate  $\Phi_{PC}$  from our measurements of  $\Phi_D$  and  $\Phi_N$ , using Eq. (2) (assuming  $\Phi_V=0$ ), as shown in panels d and h (grey regions). It can be argued

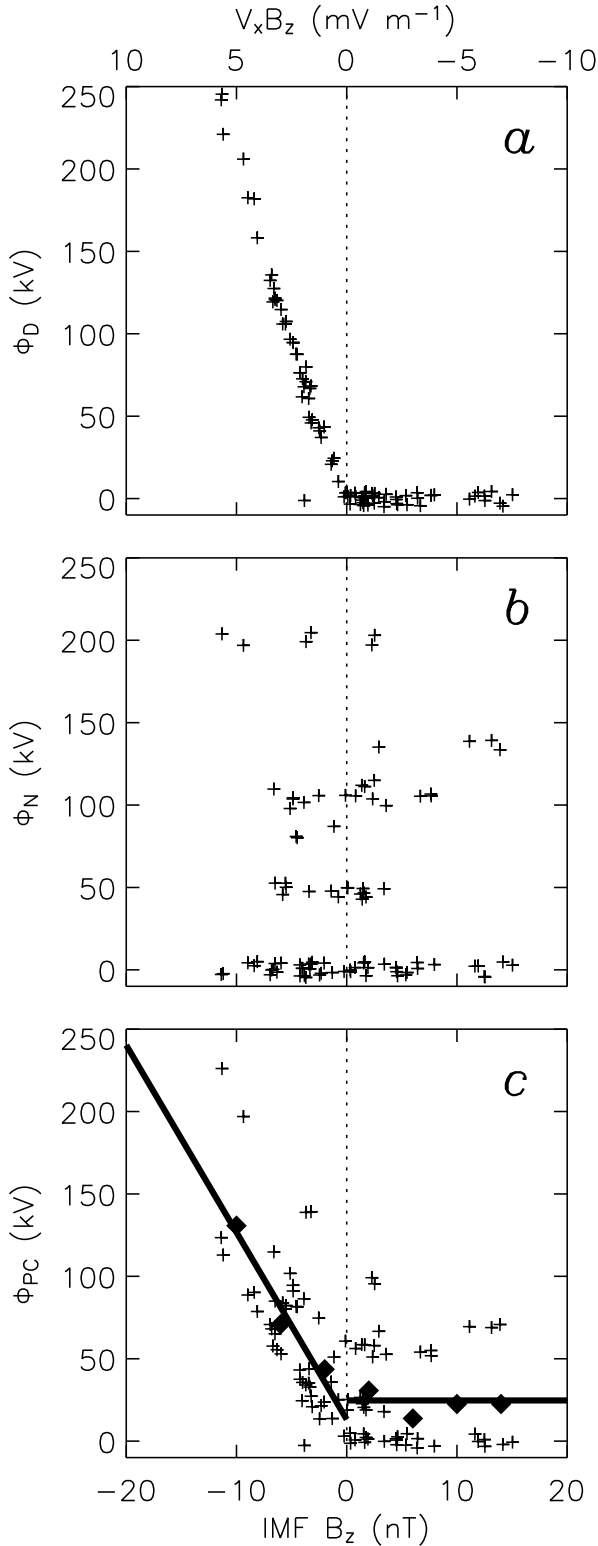


**Fig. 2.** (a) Dayside reconnection rate, (b) nightside reconnection rate, and (c) cross polar cap potential as a function of IMF  $B_z$ . In (c) solid curves show a least-squares fit in the interval  $B_z < 0$  nT, and the average value in the interval  $B_z > 0$  nT. Diamonds show average values of cross polar cap potential in 4 nT-wide bins of  $B_z$ .

that the reconfiguration of the magnetosphere, in response, to day and nightside reconnection, will have a response time of 10–15 minutes. To illustrate this we have convolved our estimates of  $\Phi_{PC}$  with a triangular response function of duration 16 min that peaks at a lag of 8 min, and indicated this by the solid curves in panels d and h. This has the effect of somewhat smoothing the response of  $\Phi_{PC}$  to the reconnection drivers. In the analysis that follows we use the unfiltered estimates of  $\Phi_{PC}$ .

Previous workers have tried to directly relate  $\Phi_{PC}$  to upstream solar wind and IMF conditions (Reiff et al., 1981, 1985; Cowley, 1984; Weimer, 2001). To reproduce the relationships found in these studies we plot  $\Phi_D$ ,  $\Phi_N$ , and  $\Phi_{PC}$  as functions of IMF  $B_z$  in Fig. 2, panels a, b, and c, respectively. These show values of a potential drop taken at 10-min intervals during the two periods under study; points have been displaced by up to  $\pm 5$  kV so that they do not all lie on top of each other.  $B_z$  can be roughly translated into the  $Y$ -component of the solar wind electric field  $E_y = V_x B_z$  (cf. Eq. (4)), assuming a mean solar wind speed of  $V_x = -500$  km/s<sup>-1</sup>.

Previous workers have employed more complicated estimates of the solar wind-magnetosphere coupling rate than solely  $B_z$  or  $V_x B_z$  but we have demonstrated that Eq. (4) works well to a first order, and wish to maintain simplicity as far as possible. As expected,  $\Phi_D$  is very closely related to  $B_z$  when  $B_z < 0$  nT (indeed, it was estimated from Eq. (4)), and is zero for  $B_z > 0$  nT.  $\Phi_N$ , on the other hand, is not correlated with  $B_z$ . Hence, the resulting  $\Phi_{PC}$  is somewhat correlated with  $B_z$  when  $B_z < 0$  nT, but is non-zero, on average, when  $B_z > 0$  nT, that is, there appears to be a spread in  $\Phi_{PC}$  at any particular value of  $B_z$ , and a residual cross polar convection remains even when no coupling is expected with the solar wind. Indeed, we find excellent agreement between our observations and the observations collated by Cowley (1984), both in the trend and spread of the data, despite considerable differences in the methods of derivation of  $\Phi_{PC}$  – directly measured by polar-orbiting spacecraft in the case of Cowley, and inferred from estimates of the day- and nightside reconnection rates in our case.

We quantify the trend and residual in two ways. The first is to perform a least-squares fit to  $\Phi_{PC}$  in the interval  $B_z < 0$  nT, and find the relationship

$$\Phi_{PC} = -11.4 B_z + 13.1, B_z < 0 \text{ nT}, \quad (5)$$

where  $\Phi_{PC}$  is expressed in kV and  $B_z$  in nT. In the interval  $B_z > 0$  nT, the mean value of  $\Phi_{PC}$  is 25 kV. These fits are shown by straight lines in Fig. 2c. The second method is to determine the mean value of  $\Phi_{PC}$  in 4 nT-wide bins of  $B_z$ , as shown by diamonds. Again, the non-zero convection residual is apparent for  $B_z > 0$  nT.

We note at this point that if Eq. (3) is employed to determine  $\Phi_{PC}$ , then a similar trend is found to that seen in Fig. 2c, though the gradient becomes  $-17$  kV nT<sup>-1</sup> for  $B_z < 0$  nT and the convection residual for  $B_z > 0$  nT rises to close to 50 kV. To more fully demonstrate the relationship

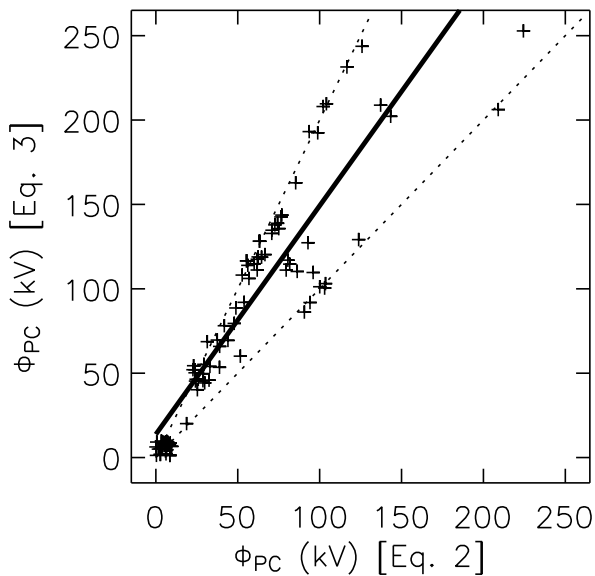


**Fig. 3.** A comparison of estimates of  $\Phi_{PC}$  from Eqs. (2) and (3). Dotted curves show the lines of  $\Phi'_{PC} = \Phi_{PC}$  and  $\Phi'_{PC} = 2\Phi_{PC}$ . The full curve shows the least-squares line of best fit.

between the two methods of calculating  $\Phi_{PC}$ , Fig. 3 presents a point-by-point comparison of Eqs. (2) and (3). Dotted curves show the line of equality ( $\Phi'_{PC} = \Phi_{PC}$ ) and the line that represents a factor of 2 difference between methods ( $\Phi'_{PC} = 2\Phi_{PC}$ ). As suggested above, many estimates from Eq. (3) are double the estimates from Eq. (2). The least-squares fit (solid curve) has a gradient of 1.4.

#### 4 Discussion

If the cross polar cap potential is considered to be the sum of two processes, one directly controlled by the upstream IMF and the other not, then it is no surprise that there remains a residual convection voltage even when dayside coupling is absent, as first suggested by Lockwood et al. (1990). This can be seen in the two examples presented in Fig. 1. During these two events the IMF is directed southwards approximately half of the time (43% and 53%, respectively). However, once nightside reconnection is taken into account,  $\Phi_{PC} = 0$  kV only 19% and 29% of the time (7% and 15% if the response function is factored in), respectively. We expect that substorm-related nightside reconnection is most likely to commence during intervals of  $B_z < 0$  nT as this is when new open flux is being added to the tail, so that an onset threshold might be exceeded in the plasma sheet. However, once tail reconnection has commenced, it can continue even after  $B_z$  has turned northward. Hence, one might expect that, on average, tail reconnection is equally as likely to be ongoing when the IMF is directed either southward or northward. There is also evidence for non-substorm episodes of tail reconnection at rates up to 30–60 kV occurring during periods of northward IMF (Grocott et al., 2003, 2004). Furthermore, in our two examples there is one case (out of 7) in which the onset

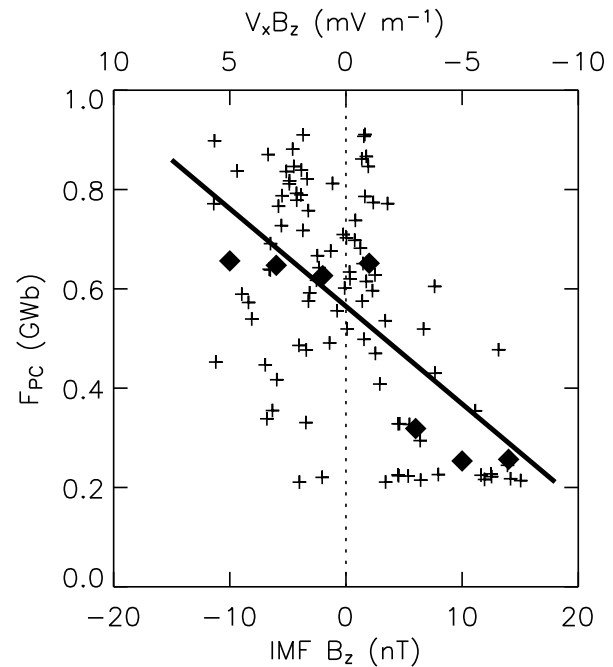


**Fig. 4.** Polar cap flux as a function of IMF  $B_z$ . The solid curve shows a least-squares fit, the diamonds show average values in 4 nT-wide bins of  $B_z$ .

of tail reconnection is externally triggered by the arrival of a solar wind shock (06:55 UT, 26 August 1998, Fig. 1e; see also Milan et al. (2004)), and this will presumably occur independently of the orientation of the IMF that is, we do not expect that there should be a bias towards tail reconnection ongoing during periods of southward or northward IMF, or in other words, the nightside reconnection rate should truly be independent of the dayside coupling rate.

The observations presented in Fig. 1 also show that the size of the polar cap, and hence the latitude at which the auroral zone is located, is not directly related to the instantaneous upstream solar wind conditions. We re-emphasize this in Fig. 4, which shows  $F_{PC}$  as a function of  $B_z$  (again at 10-min intervals). The trend is indicated in two ways: a least-squares fit to the data (solid line) and mean values of  $F_{PC}$  in 4 nT-wide bins of  $B_z$ . During periods of southward IMF the “typical” size of the polar cap may be said to be 0.65 GWb, falling to 0.3 GWb for northward IMF. However, while it is true that, on average, the polar cap is larger (and hence the oval will be expected to be located at lower latitude) for southward IMF, Fig. 4 shows that there is a great deal of spread in the size of the polar cap for any particular value of  $B_z$ . Rather, it is more accurate to say that the oval progresses to lower latitudes when the IMF is directed southwards and dayside reconnection is causing an increase in  $F_{PC}$ , and the polar cap shrinks during intervals of tail reconnection, as dictated by Eq. (1). The “typical” sizes quoted above are a consequence of changing the competition between dayside and nightside reconnection, but should only be considered as a gross temporal average of an otherwise highly dynamic system.

These results have two practical ramifications for the construction of empirical convection patterns (e.g. Heppner and Maynard, 1987; Ruohoniemi and Greenwald, 1996; Weimer, 1995, 1999, 2001). These models tend to be parameterized solely in terms of the magnitude and orientation of the upstream IMF, though this takes account of the dayside driver of convection only. It is apparent that the convection pattern will also depend significantly on substorm phase, which controls the nightside convection driver, as investigated by Weimer (1999, 2001), and clearly demonstrated by Provan et al. (2004), who conducted a super-posed epoch analysis of substorm-related convection flows. Hence, future models of convection need to be keyed to substorm phase, as well as the IMF. The convection model of Weimer (2001) does include a parameterization by auroral index AL, but this is probably not sufficient to properly characterize flows associated with different phases of the substorm cycle. In addition, we have demonstrated that the size of the polar cap, and hence the ionospheric convection pattern, is not directly related to the IMF. Hence, when each model pattern is compiled from many ionospheric observations of the convection velocity binned just by IMF orientation, the averaging process will result in considerable smearing of the true pattern, especially in the vicinity of the convection reversal boundaries (Lockwood, 1991). Models need to take into account the changing size of the polar cap during the averaging process, transforming all observations into a frame of reference determined by the current location of the open/closed field line boundary. The instantaneous size of the polar cap should also be employed to scale the convection pattern reconstructed from the IMF and substorm phase inputs. Again, this issue was addressed by Provan et al. (2004), by the use of a “shower-cap” coordinate transformation.

One further complication remains. Even after low-latitude dayside reconnection has ceased ( $IMF B_z > 0$  nT,  $\Phi_D = 0$ ) and nightside reconnection has abated ( $\Phi_N = 0$ ), it is not expected that the ionosphere should come to a standstill. Dayside reconnection can now occur at high latitudes, between the IMF and the already open field lines of the magnetotail lobes, resulting in a “reverse” convection or “lobe stirring” contained entirely within the polar cap (e.g. Cowley, 1981; Reiff and Burch, 1985). This stirring will have a voltage associated with it, of the order of a few 10s of kV (e.g. Freeman et al., 1993), and will appear as a residual flow for  $IMF B_z > 0$  nT, even though it is not associated with a net transport of flux across the polar cap. We have not estimated this in the present study as lobe stirring is not associated with a change in polar cap flux, see Eq. (1), and hence the rate of lobe reconnection cannot be determined from observations of the polar cap boundary. Suffice it to say, the existence of convective flows associated with lobe reconnection could also, in part, account for the residual flows observed for northward IMF in the past, and further reduces the need to assume a viscous interaction.

## 5 Conclusions

We have presented a new method for measuring the reconnection contribution to the cross polar cap potential, without making actual measurements of the ionospheric plasma flow. We are able to do this because of the intimate link between dayside and nightside reconnection, the creation and destruction of open flux, and the excitation of ionospheric convection (Lockwood, 1991). The results show that although the dayside driver of ionospheric convection is well-correlated with the upstream solar wind conditions, the nightside driver is not. Thus, there is a component of the convection flow that is uncorrelated with the IMF, resulting in an average residual flow of the order of 25 kV, even when the IMF is directed strongly northwards. Comparison with direct measurements of convection (e.g. Reiff et al., 1981, 1985; Weimer, 2001) which observe a residual flow of 25–35 kV, suggests that we can place an upper limit of  $\sim 10$  kV on the viscous contribution to the convection pattern. In future we intend to provide a firmer statistical footing for this work, by investigating many more intervals of data. We hope that this will also lead, for the first time, to a quantitative approach to substorm studies: for instance, regarding questions of substorm triggering, and the rate and duration of nightside flux closure.

*Acknowledgements.* SEM is supported by PPARC grant no. PPA/N/S/2000/00197. The Wind data discussed in this paper were provided by K. W. Ogilvie of NASA GSFC (Wind SWE) and R. P. Lepping and J. A. Slavin of NASA GSFC (Wind MFI), and their respective teams.

Topical Editor in chief thanks G. Chisham for his help in evaluating this paper.

## References

- Axford, W. I. and Hines, C. O.: A unifying theory of high-latitude geophysical phenomena and geomagnetic storms, *Canadian J. Phys.*, 39, 1433–1464, 1961.
- Baker, D. N., Klimas, A. J., Vassiliadis, D., Pulkkinen, T. I., and McPherron, R. L.: Re-examination of driven and unloading aspects of magnetospheric substorms, *J. Geophys. Res.*, 102, 7169–7177, 1997.
- Cowley, S. W. H.: Magnetospheric and ionospheric flow and the interplanetary magnetic field, in *The Physical Basis of the Ionosphere in the Solar-Terrestrial System*, AGARD CP-295, 4(1)–4(14), 1981.
- Cowley, S. W. H.: Solar wind control of magnetospheric convection, in *Achievements of the IMS*, ESA SP-217, 483–494, 1984.
- Cowley, S. W. H. and Lockwood, M.: Excitation and decay of solar wind-driven flows in the magnetosphere-ionosphere system, *Ann. Geophys.*, 10, 103–115, 1992.
- Dungey, J. W.: Interplanetary magnetic fields and the auroral zones, *Phys. Rev. Letters*, 6, 47–48, 1961.
- Dungey, J. W.: The structure of the exosphere or adventures in velocity space, in *Geophysics, The Earth's Environment*, eds. C. De Witt, J. Hieblot, and L. Le Beau, Gordon and Breach, New York, 503, 1963.

- Fairfield, D. H. and Cahill, L. J. Jr.: Transition region magnetic field and polar magnetic disturbances, *J. Geophys. Res.*, 71, 155, 1966.
- Freeman, M. P., Farrugia, C. J., Burlaga, L. F., Hairston, M. R., Greenspan, M. E., Ruohoniemi, J. M., Lepping, R. P.: The interaction of a magnetic cloud with the earth - ionospheric convection in the Northern and Southern Hemispheres for a wide-range of quasi-steady interplanetary magnetic-field conditions, *J. Geophys. Res.*, 98, 7633–7655, 1993.
- Heppner, J. P. and Maynard, N. C.: Empirical high-latitude electric-field models, *J. Geophys. Res.*, 92, 4467–4489, 1987.
- Holzer, R. E. and Slavin, J. A.: A correlative study of magnetic flux transfer in the magnetosphere, *J. Geophys. Res.*, 84, 2573–2578, 1979.
- Holzer, R. E., McPherron, R. L., and Hardy, D. A.: A quantitative empirical model of the magnetospheric flux transfer process, *J. Geophys. Res.*, 91, 3287–3293, 1986.
- Grocott, A., Badman, S. V., Cowley, S. W. H., Yeoman, T. K., and Cripps, P. J.: The influence of IMF  $B_y$  on the nature of the nightside high-latitude ionospheric flow during intervals of positive IMF  $B_z$ , *Ann. Geophys.*, 22, 1755–1764, 2004.
- Grocott, A., Cowley, S. W. H., and Sigwarth, J. B.: Ionospheric flow during extended intervals of northward but  $B_y$ -dominated IMF, *Ann. Geophys.*, 21, 509–538, 2003.
- Levy, R. H., Petschek, H. E., and Siscoe, G. L.: Aerodynamic aspects of the magnetospheric flow, *AIAA J.*, 2, 2065, 1964.
- Lockwood, M.: On flow reversal boundaries and transpolar voltage in average models of high latitude convection, *Planet. Space Sci.*, 3, 397–409, 1991.
- Lockwood, M. and Cowley, S. W. H.: Ionospheric convection and the substorm cycle, in *Proceedings of the International Conference on Substorms (ICS-1)*, 99–109, 1992.
- Lockwood, M., Cowley, S. W. H., and Freeman, M. P.: The excitation of plasma convection in the high latitude ionosphere, *J. Geophys. Res.*, 95, 7961–7972, 1990.
- Lockwood, M. and Freeman, M. P.: Recent ionospheric observations relating to solar wind-magnetosphere coupling, *Phil. Trans. R. Soc. A*, 328, 93, 1989.
- McPherron, R. L., Russell, C. T., and Aubry, M.: Satellite studies of magnetospheric substorms on August 15, 1968, 9. Phenomenological model for substorms, *J. Geophys. Res.*, 78, 3131–3149, 1973.
- Milan, S. E.: A simple model of the flux content of the distant magnetotail, *J. Geophys. Res.*, 109, A07210, doi: 10.1029/2004JA010397, 2004.
- Milan, S. E., Lester, M., Cowley, S. W. H., Oksavik, K., Brittnacher, M., Greenwald, R. A., Sofko, G., and Villain, J.-P.: Variations in polar cap area during two substorm cycles, *Ann. Geophys.*, 21, 1121–1140, 2003.
- Milan, S. E., Cowley, S. W. H., Lester, M., Wright, D. M., Slavin, J. A., Fillingim, M., Carlson, C. W., and Singer, H. J.: Response of the magnetotail to changes in the open flux content of the magnetosphere, *J. Geophys. Res.*, 109, A04220, doi: 10.1029/2003JA010350, 2004.
- Provan, G., Lester, M., Mende, S. B., and Milan, S. E.: Statistical study of high-latitude plasma flow during magnetospheric substorms, *Ann. Geophys.*, in press, 2004.
- Reiff, P. H. and Burch, J. L.: IMF  $B_y$ -dependent plasma flow and Birkeland currents in the dayside magnetosphere, 2. A global model for northward and southward IMF, *J. Geophys. Res.*, 90, 1595, 1985.
- Reiff, P. H., Spiro, R. W., and Hill, T. W.: Dependence of polar cap potential drop on interplanetary parameters, *J. Geophys. Res.*, 86, 7639–7648, 1981.
- Reiff, P. H., Spiro, R. W., Wolf, R. A., Kamide, Y., and King, J. H.: Comparison of polar cap potential drops estimated from solar wind and ground magnetometer data: CDAW 6, *J. Geophys. Res.*, 90, 1318–1324, 1985.
- Richmond, A. D. and Kamide, Y.: Mapping electrodynamic features of the high-latitude ionosphere from localized observations: Technique, *J. Geophys. Res.*, 93, 5741, 1988.
- Rostoker, G., Akasofu, S.-I., Baumjohann, W., Kamide, Y., and McPherron, R. L.: The roles of direct input of energy from the solar wind and unloading of stored magnetotail energy in driven magnetospheric substorms, *Space Sci. Rev.*, 46, 93–111, 1987.
- Ruohoniemi, J. M. and Baker, K. B.: Large-scale imaging of high-latitude convection with Super Dual Auroral Radar Network HF radar observations, *J. Geophys. Res.*, 103, 20 797–20 811, 1998.
- Ruohoniemi, J. M. and Greenwald, R. A.: Statistical patterns of high-latitude convection obtained from Goose Bay HF radar observations, *J. Geophys. Res.*, 101, 21 743–21 763, 1996.
- Russell, C. T.: The configuration of the magnetosphere, in *Critical Problems of Magnetospheric Physics*, ed. E. R. Dyer, Inter-Union Committee on Solar Terrestrial Physics, National Academy of Sciences, Washington, D.C., p. 1, 1972.
- Siscoe, G. L. and Huang, T. S.: Polar cap inflation and deflation, *J. Geophys. Res.*, 90, 543–547, 1985.
- Weimer, D. R.: Models of high-latitude electric potentials derived from a least error fit of spherical harmonic coefficients, *J. Geophys. Res.*, 100, 19 595–19 607, 1995.
- Weimer, D. R.: Substorm influence on the ionospheric electric potentials and currents, *J. Geophys. Res.*, 104, 185–197, 1999.
- Weimer, D. R.: An improved model of ionospheric electric potentials including substorm perturbations and application to the Geospace Environment Modeling November 24, 1996, event, *J. Geophys. Res.*, 106, 407, 2001.